Journal of Engineering and Applied Sciences 13 (20): 8360-8371, 2018
ISSN: 1816-949X

Generalize Predictive Control in Micro Grid DC System

Angie J. Valencia C., Mauricio F. Mauledoux, Edilberto Mejia Ruda,
Oscar I. Caldas and Oscar F. Aviles
Mechatronics Engineering Program, Faculty of Engineering,
Militar Nueva Granada University, Bogota, Colombia

Abstract: The energies systems are the principle challenge for the future of rural or urban society where the engineering search the solutions that make a green system for supplied the actual demand. For that the implementation of renewable energy is growing, due to lack in nature reserve, the pollution excess and the continuous demand in the use of energy to supply the necessities in the common life. It means that we need to change the way to use the environmental resources to get it using green energy sources. This research shows the results obtained by perform a generalized predictive control as one of predictive control theories in a micro grids systems because it needs few parameters and adopts strategies of multi-step prediction, receding-horizon optimization and feedback correction which has good tracking characteristic and reduces on-line calculations of control algorithm. Based on the discrete Controlled Autoregressive Integrated Moving Average (CARIMA) Model, the control algorithm was combined with merits of adaptive control which made control system possess of excellent robust and intelligent capability.

Key words: Socket, stump, stress, biomechanics, interface, principle challenge

INTRODUCTION

Actually, the current methods for energy production are not sustainable, due to environmental problematic and the lack of nature resources. This and the concerns about global warming, prevention of environmental pollution and deficiency of energy sources have been becoming important development themes in different industries. The current methods for energy production are not sustainable, mainly due to environmental reasons (McGowan *et al*., 2010).

Therefore, the demand for renewable energy, smart electrification and rational use of electricity are important factors that will provide answers to the global energy challenge. All this demand growing is also increasing the interest of how the meteorological condition play significant role in the performance of renewable energy systems whereas these systems produce optimum output under certain desired weather conditions which are essentially location.

Thus, we need apply smart grids that allows the integration of large amounts of green energy, improving reliability, quality of supply and ensuring safety in a non-interconnected zones (Shah *et al*., 2012).

Therefore and due to the great advantages and developments on renewable energy it is necessary to analyse how energy should be used in a micro-grid with renewable energy source, considering that usually the power is supplied without regard if it comes from the network or renewable supply (Alvarez-Beletal, 2013) (Chuanchuan *et al*., 2013). The current tendency is to project this type of systems to provide 80-90% of the energy needs in remote or non-electrified areas, the use of a different medium scale sources and small distance distribution such as wind and solar energy close to load, reduces local storage requirements and energy losses (Strunz *et al*. 2014).

In a smart grid system is required apply control strategies that allows get the optimum output taking to account the external conditions and applications requirements. So, it is very indispensable to find the appropriate control law which does not need high-precise model. In recent years, there are successful examples for predictive control being applied in the complicated industrial process (Ordys, 2001). Generalized Predictive Control (GPC) is one of the most important predictive control algorithm which adopted the discrete Controlled Autoregressive Integrated Moving Average (CARIMA) Model to reduce the calculation and the recursive least square algorithm with forgetting factor

Corresponding Author: Angie J. Valencia C., Mechatronics Engineering Program, Faculty of Engineering,
Militar Nueva Granada University, Bogota, Colombia

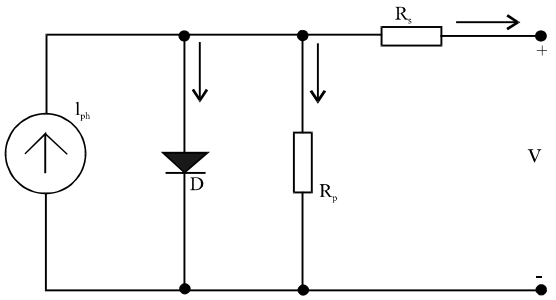

Fig. 1: Simplified model panel

to estimate the parameter model online which improve the dynamic characteristic of micro grids systems (Rodriguez and Dumur, 2005).

Therefore, this research models and simulates a DC micro grid that can get power from different centralized and renewable sources, optimizing generation and consumption. Since, forecasts never are perfect, a Generalized Predictive Control (GPC) strategy is used for keeping the consequences of forecast uncertainties at acceptable levels. This work is complemented with the micro grid implementation in Simulink-MATLAB in order to get the results of an appropriate simulation.

MATERIALS AND METHODS

Micro-grid modelling: The first models to develop in order to get the final representation in a micro-grid system is power generators as photovoltaic panels and wind turbine, followed by a storage device as batteries. Then in order to ensure consistent power to the batteries it was designed a rectifier with a buck converter which is described below.

Photovoltaic model: A Photo Voltaic (PV) module use to be represented as a two nodes electrical circuit with the sunlight generated current source (photocurrent), a diode connected in anti-parallel and both series and parallel resistances which is shown in Fig. 1 (Bellia *et al*., 2014; Ishaque *et al*., 2011).

This is a non-linear equation that includes several parameters that can be classified in three groups: those provided by the manufacturer, the electrochemical constants that can be assumed according to weather and electromechanical conditions and the ones that can be calculated.

According to the simplified model panel shown in Fig. 1, the equation that defines the PV Model dynamics in terms of an output current can obtained via. Kirchhoff's current law as shown in Eq. 1 (Parisio *et al*., 2014).

$$I = I_{ph} - I_d - I_p \quad (1)$$

where, I_{ph}, I_d and I_p are defined in the Eq. 2-4, respectively.

$$I_{ph} = \frac{G}{G_{ref}}(I_{ph,\,ref} + \mu_{sc}\Delta T) \quad (2)$$

$$I_d = I_o\left[\exp\left(\frac{V+IR_s}{a}\right)-1\right] \quad (3)$$

$$I_p = \frac{V+IR_s}{v} \quad (4)$$

Where:

G = The irradiance
G_{ref} = The irradiance at standard test conditions
T_c = The cells temperature, thus, $T = Tc - T_{c,ref}$ (T_c = 298 k)
μ_{sc} = The coefficient temperature of short circuit current (given by the manufacturer)

Wind turbine model: This study describes the modelling of a wind turbine and the simplified model of the blades. In order to model a wind turbine it must be considered a load to which the blades can react in various ways and then have more than twenty degrees of freedom in their reaction.

This section starts defining the static and mechanical characteristics. The Tip-Speed Ratio (TSR), denoted by λ is the radio between the linear speed of the tip of the blade to the wind speed as is shown in Eq. 5. This can be calculated by means of the rotor radius and angular speed (Weimer *et al*., 2006):

$$\lambda = \frac{r_r w_r}{V_w} \quad (5)$$

The TSR and the user-defined blade pitch angle are used to calculate the rotor power coefficient, denoted by C_p (Tang *et al*., 2011). This coefficient is a measure of the rotor efficiency and is defined as is shown in Eq. 6:

$$C_p = \frac{P_r}{P_w} \quad (6)$$

Where:

P_w = Defined as the power of wind
P_r = The power of rotor

Finally, the state equation is presented in the Eq. 7 and 8.

$$\begin{bmatrix} \dot{\omega}_{re}^{*} \\ \dot{\theta}_{re}^{*} \\ \dot{i} \end{bmatrix} = \begin{bmatrix} -\frac{r}{r} & & \\ 1 & 0 & 0 \\ \frac{L}{L} & 0 & -\frac{R}{L} \end{bmatrix} \begin{bmatrix} \omega_{re} \\ \theta_{re} \\ i \end{bmatrix} + \begin{bmatrix} -\frac{}{re} \\ 0 \\ 0 \end{bmatrix} [T_r] \quad (7)$$

$$y = [0 \;\; 0 \;\; 1] \begin{bmatrix} w_{re} \\ \theta_{re} \\ i_g \end{bmatrix} \quad (8)$$

Battery model: The battery block implements a generic dynamic model parameterized to represent most popular types of rechargeable batteries. The model can be expressed by the Open Circuit Voltage (OCV) or Electro Motive Force (EMF) E_0, the voltage in the terminals of the battery V_t, the internal resistance R_i, the discharge current I and the State of Charge (SOC) Q as shown in Eq. 9 and 10 (Parisio *et al*., 2014):

$$E = E_0 - K\frac{Q}{Q - \int idt} + A_e^{-B\int idt} \quad (9)$$

$$V_t = E - R_{ii} \quad (10)$$

Where:
Q = The maximum battery capacity
A = The exponential zone amplitude
K = The polarization voltage constant and
B = The exponential zone time constant inverse capacity

The battery voltage obtained is given by Eq. 11:

$$E_{batt} - E_0 - K\frac{Q}{Q-it} - R_i - K\frac{Q}{Q-i}i^* + A_e^{-Bit} \quad (11)$$

Where:
it = Means the current battery voltage
I* = The filtered current

Buck converter model: The typology of buck converter is shown in Fig. 2 in which the power switch S inductor L and Capacitor C constitute the conventional buck converter. The Resistance R represents the load on the battery circuit and it is simulated as a time-variant varying signal (Parisio *et al*., 2014). The dynamic process of the circuit can be described by the ordinary differential (Eq. 12 and 13).

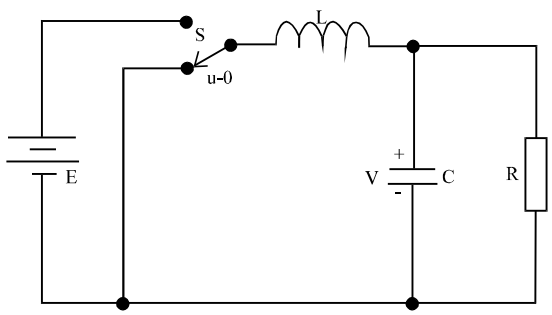

Fig. 2: Buck converter diagram

$$L\frac{di}{dt} = -v + Eu \quad (12)$$

$$C\frac{dv}{dt} = i - Rv \quad (13)$$

Micro-grid system: The prototype micro-grid was proposed to be modelled as is shown in Fig. 3. The first developed models were a photovoltaic panel, wind turbine and battery bank. Also in order to ensure consistent power to the battery bank it was designed a rectifier with a buck converter.

The structure of the photovoltaic block model is define by a two nodes electrical circuit with the sunlight generated current source and the wind turbine structure must be considered a load with blades that can react in a lot of ways with more than 20° of freedom in their reaction. The battery model can be expressed by the Open Circuit Voltage (OCV) or Electro Motive Force (EMF) in order to get a dynamic model to represent most popular types of rechargeable batteries. Finally, the typology of buck converter is represented by a power switch inductor and capacitor, like a conventional buck converter (Pati *et al*., 2016).

After obtaining the individual renewable source model representation, we integrated it into the micro grid system to get the final mathematical model in this case is required apply linearization techniques that provides us with a lot of insight about its dynamics because the complexity of the system does not reveal the total integration dynamic with renewable sources using difference equations.

MATLAB provide a linear analysis tool that helps us with the linearization model using the simulink representation as is shown in the Fig. 3. In this tool is required define the operating point in this case we use the model initial conditions as is shown in the Table 1.

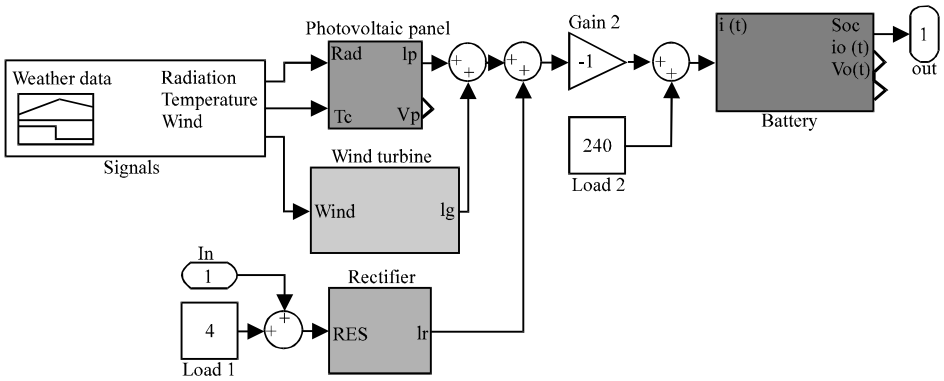

Fig. 3: Micro grid representation

Table 1: Model initial conditions

Condition	Values
Wind turbine	0.0001
Battery model	498960
Buck converter	1
Photovoltaic panel	0

Then, the tool give us the space state, the zero pole gain and the transfer function representation but we use the transfer function in Eq. 14 in order to calculate a generalized predictive control:

$$G(z)=\frac{1.474*10^{-5}z^5-5.826*10^{-6}z^4-3.998*10^{-6}z^3+2.052*10^{-6}z^2+2.573*10^{-7}z+1.848*10^{-13}}{z^6-2.089z^5+1.46z^4-0.3732z^3+0.0002089z^2-1.641*10^{-9}z+6.203*10^{-14}} \quad (14)$$

Then, we make the linear analysis again in order to obtain the transfer function of measurement disturbances model as is shown in Eq. 15:

$$G(z)=\frac{-0.00098^5z^5+0.000889^6z^4+0.000473^6z^3+6.094*10^{-5}z^2+0.000344^5z-0.0001481}{z^6-2.08^9z^5+1.46z^4-0.3732z^3+0.0002089z^2-1.641*10^{-9}z+6.203*10^{-14}} \quad (15)$$

CARIMA Model in a GPC: The most common SISO transfer function model in GPC is the CARIMA Model because it considered the uncertainty that could have a non-zero steady state in its representation, so, in Eq. 16 is shown the mathematical expression of this model. Where ς_k means a random variable and T(z) is treated as a design parameter. For convenience the CARIMA Model can be expressed as is shown in the Eq. 17 where [a(z)Δ] is a combination between a (z) and delta (Δ) and Δu_k use input increments with[15] $\Delta = 1-z^{-1}$.

$$a(z)y_k = b(z)u_k + T(z)\frac{\varsigma_k}{\Delta} \quad (16)$$

$$[a(z)\Delta]y_k = b(z)[\Delta u_k] + T(z)\varsigma_k \quad (17)$$

Another way to represented the CARIMA Model is through the Eq. 18 where A(z) is equal to $a(z)\Delta$. In SISO Models the b(z) and A(z) are given by the numerator and denominator as is shown in Eq. 19 and 20, respectively:

$$A(z)y_k = b(z)[\Delta uk] + T(z)\varsigma_k \quad (18)$$

$$b(z) = b_1z^{-1} + , \ldots, + b_mz^{-m} \quad (19)$$

$$A(z) = 1 + A_1z^{-1} + , \ldots, + A_nz^{-n} \quad (20)$$

The one-step ahead predictions can be used recursively to find a n-steps ahead predictions as is shown in the Eq. 21. The recursively concept is interpreted as follows: We have used the one step ahead to find y_{k+1}, the substitute it into the next equation to find y_{k+2}, then use y_{k+1} and $y_{k=2}$ to determine y_{k+z} and keep iterating until get the n-steps predictions.

$$y_{k+3} + , \ldots, + A_ny^{k-n+3} = b_1\Delta u_{k+2} + , \ldots, + b_m\Delta u_{k-m} + 3@y_{k+4} + , \ldots, + A_ny_{k-n+4} = b \quad (21)$$

The previous equations can be represented in a shorthand notation using matrix and vector format in order to separate the past and future variables as is show in Eq. 22:

$$C_A y_{-k+1} + H_A y\text{-}k = Cb_{\rightarrow}^{\Delta_{uk}} + Hb_{\leftarrow}^{\Delta_{uk-1}} \quad (22)$$

Solving the output prediction using the shorthand format, we obtain the y_{k+1} value in future input increments and past data terms as is sown in Eq. 23 where $H = C_A^{-1}C_b$, $P = C_A^{-1}H_b$ and $Q = C_A^{-1}H_A$.

$$y_{k+1} = H_{\rightarrow}^{\Delta_{uk}} + P_{\leftarrow}^{\Delta_{uk-1}} \text{-} Qy\text{-}k \quad (23)$$

Note: The H, P and Q matrix dimension are determinates by the prediction and control horizons.

Control law: The first step in the develop of a GPC law algorithm is define the unbiased cost (J) as is shown in Eq. 24 where $e_{k+1} = r_{k+1}|y_{k+1}$ and γ is a constant value between 0 and 1 that determines the controller robustness (Zhou and Qu, 2016):

$$J = e_{\rightarrow k+1}^{T} e_{k+1} + \lambda \Delta u_{\rightarrow k}^{T} \Delta u_{\rightarrow k} \quad (24)$$

Consequently, we can perform a minimization to find the optimum J value. So, taking into account the Eq. 23 is necessary replace it on the last equation to obtain the Eq. 25 in order to get a representation with the past and future values as is shown in the Eq. 26 where the first two rows represents the past Δu values and the last two rows represents the future Δu values:

$$\begin{aligned} J = {} & \left[r_{\rightarrow k+1}^{T} \text{-} H_{\rightarrow}^{T\Delta_{uk}} \text{-} P_{\leftarrow}^{T\Delta_{uk-1}} + Q^{T} y_{-k} \right] \\ & \left[r_{\rightarrow k+1} - H_{\rightarrow}^{\Delta_{uk}} - P_{\leftarrow}^{\Delta uk-1} + Q^{T} y_{\leftarrow -k} \right] + \\ & \lambda \Delta u_{\rightarrow k}^{T} \Delta u_{\rightarrow k} \left[r_{\rightarrow k+1}^{T} \text{-} P_{\leftarrow}^{T\Delta_{uk-1}} + Q^{T} y_{-k} \right] \\ & \left[r\text{-}k\text{+}1\text{-}P_{\leftarrow}^{\Delta_{uk-1}} + Qy\text{-}k \right] + \end{aligned} \quad (25)$$

$$\begin{aligned} J = {} & \left[\left(H_{\rightarrow}^{\Delta_{uk}} \right)^{T} \right] \cdot \left[H_{\rightarrow}^{\Delta_{uk}} \right] \text{-} \left[2 \left(H_{\rightarrow}^{\Delta_{uk}} \right)^{T} \right] \\ & \left[r_{-k+1} \text{-} P_{\leftarrow}^{\Delta_{uk-1}} + Qy\text{-}k \right] + \lambda \Delta u_{-k}^{T} \Delta u_{-k} \end{aligned} \quad (26)$$

Considering the previous equation we can eliminate the past terms because they not affect the values that should be minimized in the optimization rule.

In the optimization of the unbiased cost J exist an only minimum determinates by a gradient equal zero. For the previous reason the optimum equation is given by Eq. 27:

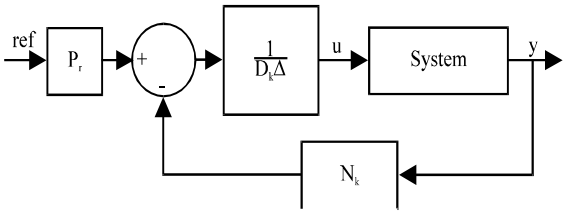

Fig. 4: Block diagram general predictive control

$$\left(H^{T}H + \lambda I \right)^{-1} H^{T} \Delta u_{-k} = \left[r_{-k+1} \text{-} P_{\leftarrow}^{\Delta_{uk-1}} + Qy\text{-}k \right] \quad (27)$$

The control law equation is determinate by a k constant defines by the first row of matrix $(h^{T}H+\lambda I)^{-1}H^{T}$ multiply by Δu_{-k} as is shown in the Eq. 28 (Hou *et al*., 2014):

$$k.(H^{T}H + \lambda I)^{-1} H^{T} \Delta u_{k} = \left[r_{-k+1} \text{-} P_{\leftarrow}^{\Delta_{uk-1}} + Qy\text{-}k \right] \quad (28)$$

To make a block diagram simulation is required unpack each term of the u_k equation in vectors as is shown in the Eq. 29. Where the number of terms in the vector P_r are define by the prediction horizon, the number in the vector D_k are define by the number of terms in model numerator and finally the number of terms in the vector N_k are define by the model denominator. Then the GPC control law is summarised as is shown in Eq. 30:

$$\begin{aligned} P_r &= k.\left(H^{T}H + \lambda I \right)^{-1} H^{T} \\ D_k &= P_r\, P \\ Nk &= P_r\, Q \end{aligned} \quad (29)$$

$$\Delta u_k = P_r\, r_{-k+1} + D_k \Delta u_k \text{-} N_k y_{-k} \quad (30)$$

Grouping common terms we obtain the Eq. 27. A more conventional equation form could be written as is shown in the Eq. 32. Then, we can use this equation to get the block diagram to be implemented in the Simulink model as is show in the Fig. 4:

$$(1\text{-}D_k)\Delta u_k = P_r\, r_{-k+1} \text{-} N_k y_{-k} \quad (31)$$

$$u_k = \left[(1\text{-}D_k)\Delta \right]^{-1} (P_r\, r_{-k+1} \text{-} N_k y_{-k}) \quad (32)$$

Finally, we implemented the control structure in the prototype micro-grid representation in order to get the final block diagram as is shown in the Fig. 5.

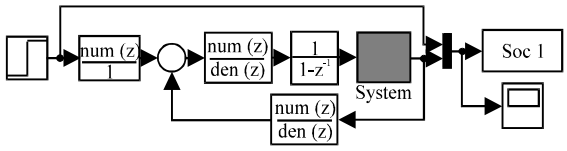

Fig. 5: Prototype Micro-Grid and GPC control

CARIMA Model in a GPC with measurement disturbances model: Using CARIMA Model, the new representation considering measurement disturbances model is shown in Eq. 33:

$$a(z)y_k = b(z)u_k + d(z)v_k + T(z)\frac{\varsigma_k}{\Delta} \tag{33}$$

where, $d(z)v_k$ is the representation of disturbances transfer function. For convenience, the CARIMA Model can be expressed as is shown in Eq. 34 where $[a(z)\Delta]$ is a combination between a(z) and delta (Δ), Δu_kuse input increments and Δv_k use disturbances increments with[15] $\Delta = 1\text{-}z^{-1}$:

$$[a(z)\Delta]y_k = b(z)[\Delta u_k] + d(z)[\Delta v_k] + T(z)\varsigma_k \tag{34}$$

Another way to represent the CARIMA Model is through the Eq. 35. In SISO Models the b (z) and A(Z) are given by the numerator and denominator as is shown in Eq. 36 and 37, respectively. While d (z) are given by the numerator of disturbance model as is shown in Eq. 38 (Chen *et al*., 2008):

$$A(z)y_k = b(z)[\Delta u_k] + d(z)[\Delta v_k] + T(z)\varsigma_k \tag{35}$$

$$b(z) = b_1 z^{-1} +, ..., +b_m z^{-m} \tag{36}$$

$$A(z) = 1 + A_1 z\text{-}1 +, ..., + A_n Z^{-n} \tag{37}$$

$$d(z) = d_0 + d_1 z^{-1} +, ..., d_p z^{-p} \tag{38}$$

In this step we use the same recursively concept integrated the d (Z). To have an appropriate notation we considering the system in terms of matrix and vectors as is shown in Eq. 39:

$$y_{k-1} = H^{\Delta}_{\rightarrow}u_k + P^{\Delta}_{\leftarrow}u_{k-1} + E^{\Delta}_{\rightarrow}v_k + G^{\Delta}_{\leftarrow}v_{k-1} - Qy_{-k} \tag{39}$$

Where:

H = $C_A^{-1}C_b$

P = $C_A^{-1}H_b$, = $C_A^{-1}C_d$

G = $C_A^{-1}H_d$ yQ = $C_A^{-1}H_A$

Note: The H, P, E, G and Q, matrix dimension are determinates by the prediction and control horizons.

Control law: We have to consider the same unbiased cost showed in Eq. 24. Consequently, we can perform a minimization to find the optimum J value. So, taking into account the Eq. 39 is necessary replace it in order to get a representation with the past and future values as is shown in Eq. 40:

$$\begin{aligned} J = {} & \left(r_{(\rightarrow k+1)}\right)^T - P^T(\Delta @ \leftarrow)u_{(k-1)} - \\ & E^T(\Delta @ \rightarrow)v_k - G^T(\Delta @ \leftarrow)v_{(k-1)} + \\ & Q^T y_{(\leftarrow k)} @ \left[r_{(k+1)} - P(\Delta @ \rightarrow)v_k - G(\Delta @ \leftarrow)\right] \end{aligned} \tag{40}$$

Considering the previous equation we can eliminate the past terms because they not affect the values that should be minimized in the optimization rule.

In the optimization of the unbiased cost J exist an only minimum determinates by a gradient equal zero. For the previous reason the optimum equation is given by Eq. 41:

$$\begin{aligned} & \left(H^T H + \lambda.1\right)^{-1} H^T \\ & \Delta u_{\rightarrow}k = \left[r_{\rightarrow}k + 1 - P^{\Delta}_{\rightarrow}u_{k-1} - E^{\Delta}_{\rightarrow}v_k - G^{\Delta}_{\leftarrow}v_{k-1} + Qy_{\leftarrow k}\right] \end{aligned} \tag{41}$$

The control law equation is determinate by a k constant defines by the first row of matrix $(HTH+ \lambda I)^{-1}H^T$ multiply by Δu_{-k} as is shown in Eq. 42 (Hou *et al*., 2014):

$$\begin{aligned} & k.\left(H^T H + \lambda.1\right)^{-1} H^T \\ & \Delta u_{\rightarrow}k = \left[r_{\rightarrow}k + 1 - P^{\Delta}_{\rightarrow}u_{k-1} - E^{\Delta}_{\rightarrow}v_k - G^{\Delta}_{\leftarrow}v_{k-1} + Qy_{\leftarrow k}\right] \end{aligned} \tag{42}$$

To make a block diagram simulation is required unpack each term of the u_k equation in vectors as is shown in Eq. 43. Then the GPC control law is summarized as is shown in Eq. 44:

$$\begin{aligned} P_r &= k.\left(H^T H + \lambda.1\right)^{-1} H^T \\ D_k &= P_r P \\ N_k &= -P_r Q \\ R_k &= P_r E \\ S_k &= P_r G \end{aligned} \tag{43}$$

$$\Delta u_k = P_r r \rightarrow k+1 - D_k \Delta u_k - R_{k\rightarrow}^{\Delta} v_{k+1} - s_{k\leftarrow}^{\Delta} v_k - N_k y_{\leftarrow k} \tag{44}$$

The final representation u_k is shown in Eq. 45:

$$u_k = \left[(1-D_k)\Delta\right]^{-1}\left(p_r r_{\leftarrow k+1} - R^{\Delta}_{k\rightarrow} v_{k+1} - s_{k\rightarrow}^{\Delta} v_k - N_k y_{\leftarrow k}\right) \quad (45)$$

T-filter in a GPC: This filter makes a reduction in a high frequencies with some loses in low frequencies without change the poles system behaviour (Rossiter, 2014). To integrate the filter in a GPC diagram we begins from Eq. 46:

$$\bar{y}_{k+1} = H^{\Delta}_{\rightarrow}\overline{u_k} + P^{\Delta}_{\leftarrow}\bar{u}_{k-1} + E^{\Delta}_{\rightarrow}\bar{v}_{k+1} + G^{\Delta}_{\leftarrow}\bar{v}_k - Q^{\bar{y}k}_{\leftarrow} \quad (46)$$

Then, we use the matrices Toeplitz/Hankel to make the relationship between system without and with filter as is shown in Eq. 47 (Rossiter, 2014):

$$C_{Tk+1}\tilde{y} + H^{\square}_{T\rightarrow} = y_{k+1} \quad (47)$$

Using the previous equation, we solve the predictions in Eq. 48 in order to obtain the filters values of $\Delta\tilde{u}_k$ in Eq. 49 and $\Delta\tilde{v}_{k+1}$ in Eq. 50:

$$\tilde{y}_{k+1} = C_T^{-1}\left[y_{k+1} - H_{T\rightarrow}^{\tilde{y}k}\right] \quad (48)$$

$$\overline{{}^{\Delta}_{\rightarrow}u_k} = C_T^{-1}\left[{}^{\Delta}_{\rightarrow}u_k - H_{T\rightarrow}^{\tilde{y}k}\right] \quad (49)$$

$${}^{\Delta}_{\rightarrow}\tilde{v}_{k+1} = C_T^{-1}\left[{}^{\Delta}_{\rightarrow}\tilde{v}_{k+1} - H_{T\rightarrow}^{\tilde{y}k}\right] \quad (50)$$

Finally, we obtain the predictions in term of filtered and unfiltered data as is shown in Eq. 51:

$$y_{k+1} = H^{\Delta}_{\rightarrow}u_k + \left[C_T P - HH_T\right]^{\Delta}_{\leftarrow}\bar{u}_{k-1} + E^{\Delta}_{\rightarrow}v_{k+1} + \left[C_T G - EH_T\right]^{\Delta}_{\leftarrow}\bar{v}_k - \left[C_T Q - H\right]^{\bar{y}_k}_{\leftarrow} \quad (51)$$

Considering an appropriate nomenclature, we use, $P_t = [C_T P\text{-}HH_T]$, $G_t = [C_T G\text{-}EH_T]$ y $Q_t = [C_T Q+H]$ and $\tilde{D}_k, \tilde{S}_k, y\tilde{N}_k$, defined in Eq. 52. Taking into account that $\Delta\tilde{u} = \Delta u / T$ and $\tilde{y} = y / T$ we obtain the new signal control representation as is shown in Eq. 53:

$$\begin{aligned}\tilde{D}_k &= P_r P_t \\ N_k &= -P_r Q_t \\ \tilde{S}_k &= P_r G_t\end{aligned} \quad (52)$$

$$u_k = \left[\frac{\square}{T}\Delta\right]^{-1}\left[P_r \xrightarrow{r_{k+1}} - R_{k\rightarrow}^{\Delta}\bar{v}_{k+1} - \frac{\tilde{S}_k}{T_{\rightarrow}}^{\Delta}\bar{v}_k - \frac{\overline{N_k}}{T_{\leftarrow}}^{\bar{y}_k}\right] \quad (53)$$

RESULTS AND DISCUSSION

Below it we simulate the GPC behaviour we use the diagram in the Fig. 6. Considering the previous diagram, we make the block simulation in Simulink/MATLAB as is shown in Fig. 7. We proposed a control block with matrices P_r, D_k and N_k, follwed by a sitch block that allows the battery charge when it need it and network feed when the batteries are totally charged. We can found the rectifier block that allows give the current necessary to charge the batteries. Finally it is the battery system with measurement disturbances.

To make the control system we use a control horizon of 50 and prediction horizon of 100 with a lambda of 0.5 and a filter of (1-0.01). We obtained as result a charge battery behaviour showed in Fig. 8 without disturbances with a signal control given in Fig. 9 and rectifier response given in Fig. 10.

This controller show a desired response when we want charge the battery at 80% with an initial peak eliminated after 1, 4-10^4 sec. The rectifiers system show a current with values of 450A in the initial control signal to reach the reference quickly, then it is stabilize in 200A in order to maintain the battery in the desired level. When the disturbances are considered, we obtain the system, control and rectifier behaviour showed in Fig. 11-13, respectively.

When the disturbances are applied, the controller mitigate the disturbances but it has some peaks due to it do not implemented a disturbances model.

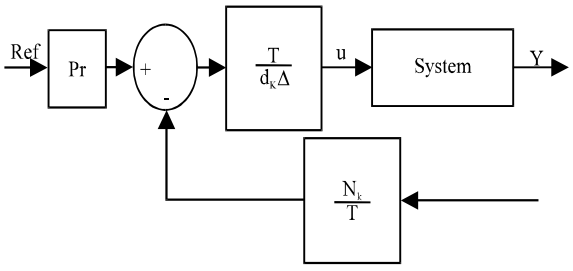

Fig. 6: GPC controller simulation diagram

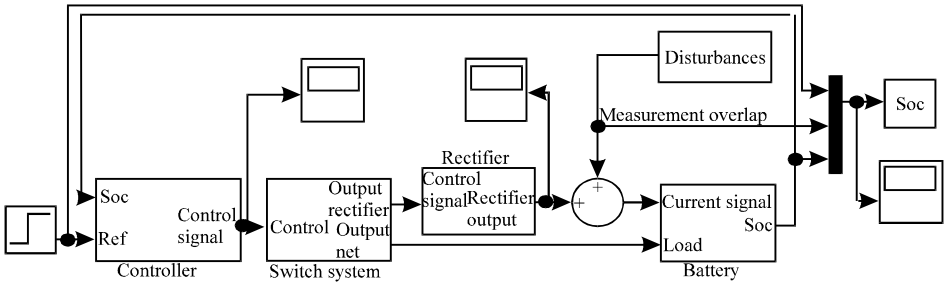

Fig. 7: Micro-grid control diagram

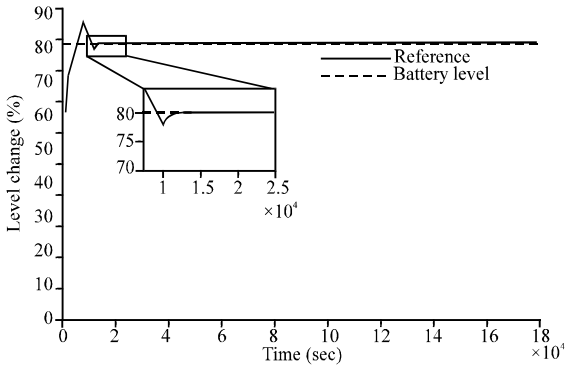

Fig. 8: Behaviour of battery charge

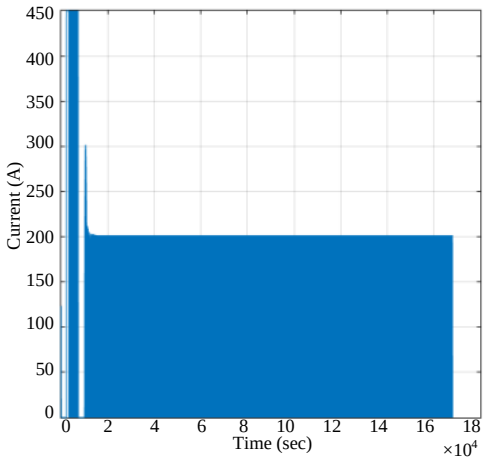

Fig. 9: Control signal without disturbances

Obtained the behaviour of GPC without disturbances model, we continues with GPC with disturbances model, so, we used the diagram in the Fig. 14.

When the disturbances are applied, the controller mitigate the disturbances but it has some peaks due to it do not implemented a disturbances model.

Obtained the behaviour of GPC without disturbances model, we continues with GPC with disturbances model, so, we used the diagram in the Fig. 15.

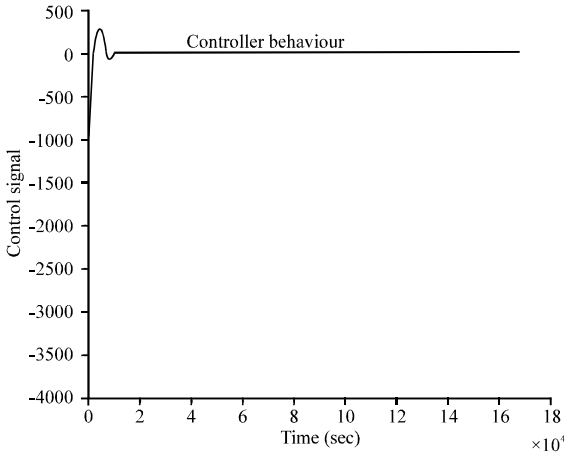

Fig. 10: Rectifier signal without disturbances

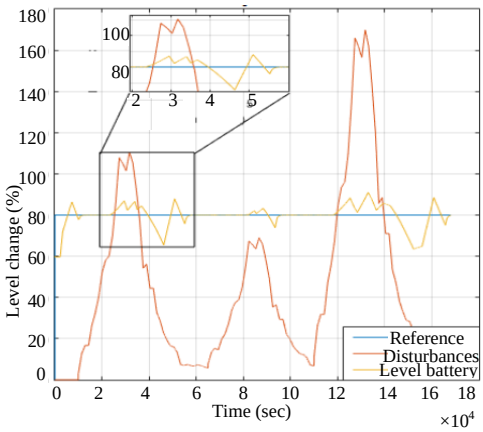

Fig. 11: Behaviour of battery charge

To make the control system we use a control horizon of 10 and prediction horizon of 110 with a lambda of 1.10^{-8} and a filter of (1, -0.001). We obtained as result a chargebattery behaviour showed in Fig. 16 without disturbances with a signal control given in Fig. 17 and rectifier response given in Fig. 18.

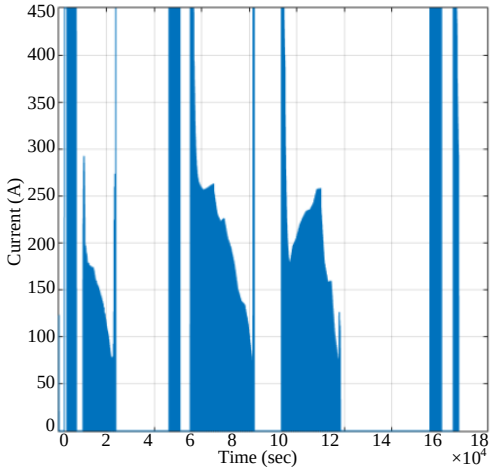

Fig. 12: Control signal with disturbances

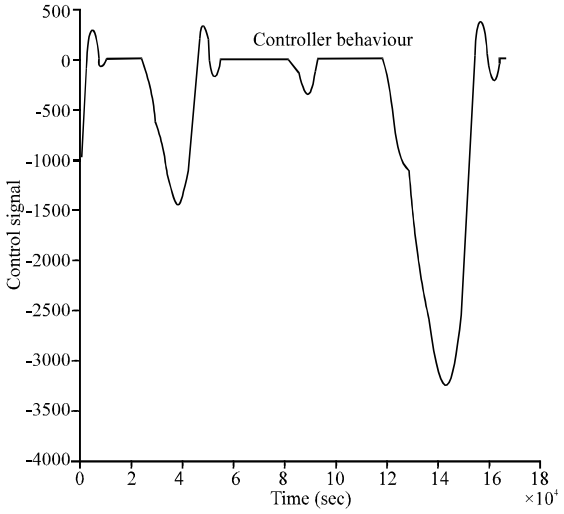

Fig. 13: Rectifier signal with disturbances

The previous controller show an efficient response because it do not has peaks to stabilize the system into the reference, besides it reach the reference in a minimum time when is compared with the controller without disturbances model.

When the disturbances are considered, we obtain the system, control and rectifier behaviour showed in Fig. 19-21, respectively.

The final response shows a controller able to mitigate the disturbances easier due to it has the disturbances model contemplate into the general control structure, showing an excellent controller to be apply in this kind of applications.

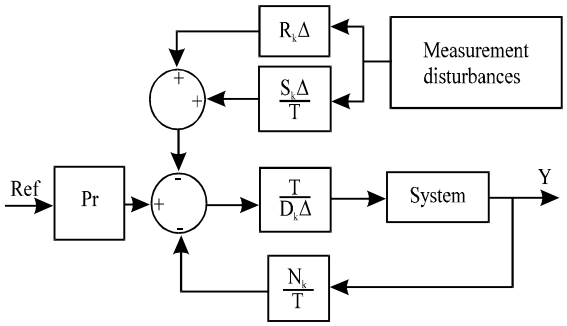

Fig. 14: Disturbance model in a GPC diagram

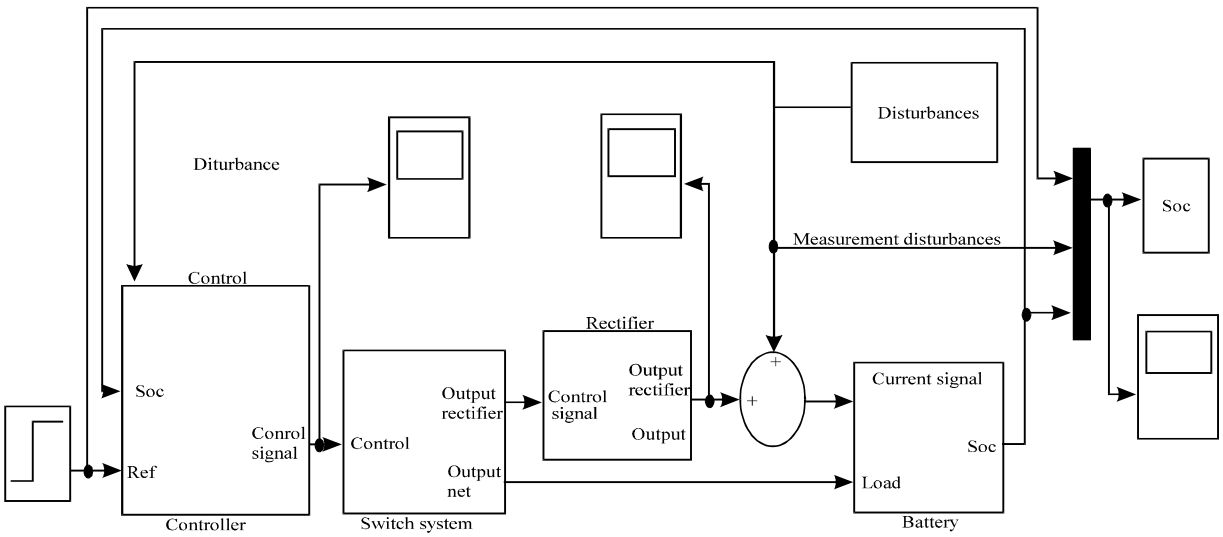

Fig. 15: Disturbance model in a micro-grid system

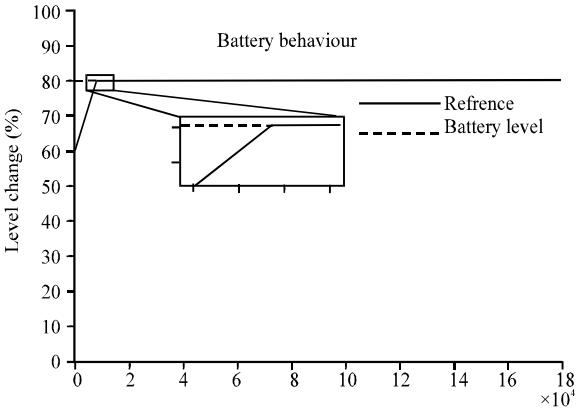

Fig. 16: Behaviour of battery charge

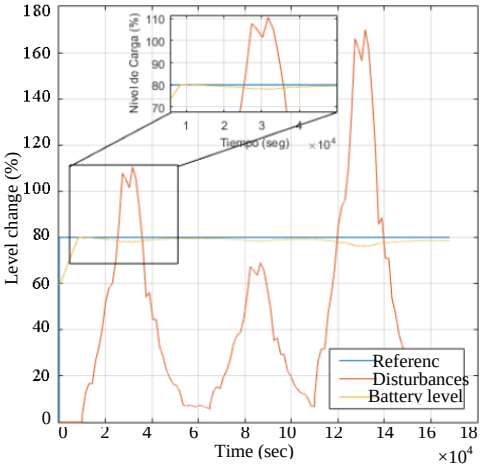

Fig. 19: Behaviour of battery charge

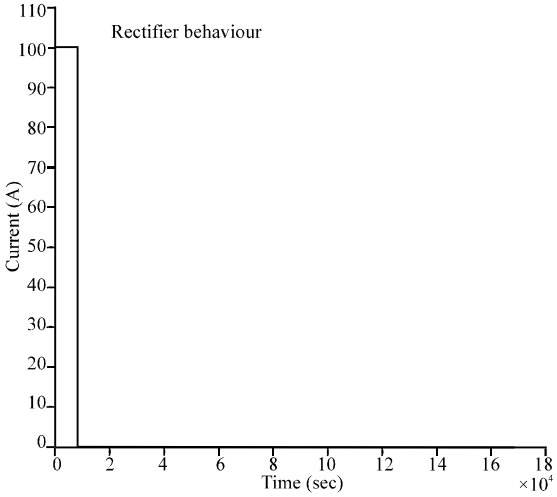

Fig. 17: Control signal without disturbances

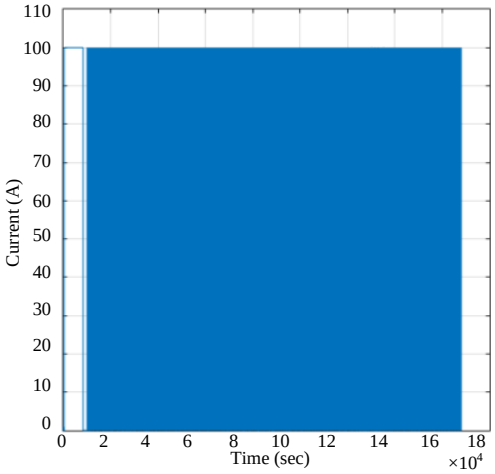

Fig. 20: Rectifier signal with disturbances

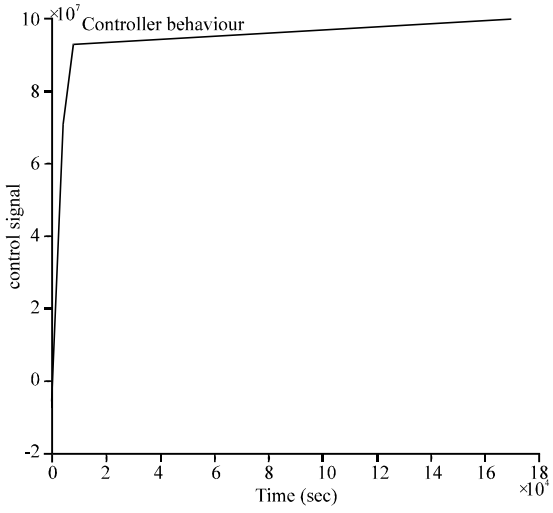

Fig. 18: Rectifier signal without disturbances

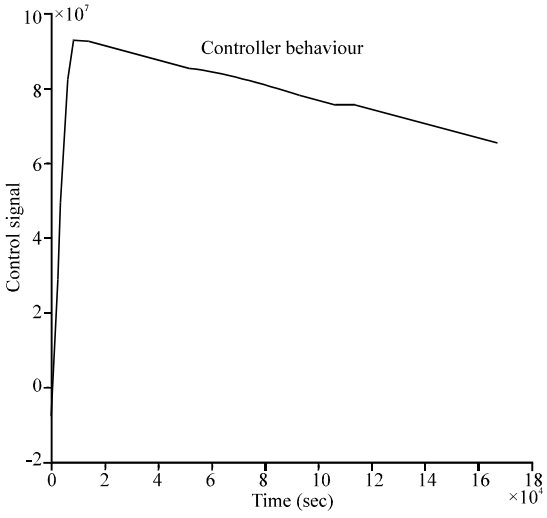

Fig. 21: Control signal with disturbances

CONCLUSION

The aim of this research was obtain a GPC controller able to get the desired behaviour in the battery level charge to a micro-grid system. As a main factor we contemplate a development of a code that provide us the ability to embedded it in a board in order to obtain a physical system to be integrated in a real micro-grid.

Thus, we design a controller based on generalize predictive techniques that give us as result a good controller to be applied in order to charge a battery in a desired reference, considering the disturbances like the energy given by a photovoltaic panel and wind turbines.

ACKNOWLEDGEMENTS

This research was financially supported by the Vice-presidency of Research at Nueva Granada Military University, through the project ING-1577 titled "Development, automation and control of a hybrid renewable resources plant" (2014-2015).

REFERENCES

Alvarez-Bel, C., G. Escriva-Escriva and M. Alcazar-Ortega, 2013. Renewable generation and demand response integration in micro-grids: Development of a new energy management and control system. Energy Effic., 6: 695-706.

Bellia, H., R. Youcef and M. Fatima, 2014. A detailed modeling of photovoltaic module using MATLAB. Nriag J. Astron. Geophys., 3: 53-61.

Chen, G.Y., P. Ren and H.L. Pei, 2008. An improved PID generalized predictive control algorithm. Proceedings of the 2008 International Conference on Machine Learning and Cybernetics Vol. 4, July 12-15, 2008, IEEE, Kunming, China, ISBN:978-1-4244-2095-7, pp: 1877-1881.

Chuanchuan, C., Z. Jun and J. Panpan, 2013. Multi-agent system applied to energy management system for renewable energy micro-grid. Proceedings of the 5th International Conference on Power Electronics Systems and Applications (PESA'13), December 11-13, 2013, IEEE, Hong Kong, ISBN:978-1-4799-3492-8, pp: 1-6.

Hou, G., X. Bai and R. Huang, 2014. Application of improved generalized predictive control to coordinated control system in supercritical unit. Proceedings of the 2014 IEEE 9th Conference on Industrial Electronics and Applications (ICIEA'14), June 9-11, 2014, IEEE, Hangzhou, China, ISBN:978-1-4799-4314-2, pp: 1591-1595.

Ishaque, K., Z. Salam and H. Taheri, 2011. Modeling and simulation of photovoltaic (PV) system during partial shading based on a two-diode model. Simul. Modell. Pract. Theory, 19: 1613-1626.

McGowan, J.G., A.L. Rogers and J.F. Manwell, 2010. Wind Energy Explained: Theory, Design and Application. 2nd Edn., John Wiley & Sons, Hoboken, New Jersey, USA., ISBN:978-0-470-01500-1, Pages: 689.

Ordys, A.W., 2001. Predictive control for industrial applications. Ann. Rev. Control, 25: 13-24.

Parisio, A., E. Rikos and L. Glielmo, 2014. A model predictive control approach to microgrid operation optimization. IEEE. Trans. Control Syst. Technol., 22: 1813-1827.

Pati, S., K.B. Mohanty, S.K. Kar and D. Panda, 2016. Voltage and frequency stabilization of a micro hydro-PV based hybrid micro grid using STATCOM equipped with battery energy storage system. Proceedings of the 2016 IEEE International Conference on Power Electronics, Drives and Energy Systems (PEDES'16), December 14-17, 2016, IEEE, Trivandrum, India, ISBN:978-1-4673-8889-4, pp: 1-5.

Rodriguez, P. and D. Dumur, 2005. Generalized predictive control robustification under frequency and time-domain constraints. IEEE. Trans. Control Syst. Technol., 13: 577-587.

Rossiter, A., 2014. The T-filter in GPC. Open Engineering Resources, Loughborough, UK.

Shah, K., P. Chen, A. Schwab, K. Shenai and S. Gouin-Davis *et al*., 2012. Smart efficient solar DC micro-grid. Proceedings of the Conference on Energytech, May 29-31, 2012, IEEE, Cleveland, Ohio, USA., ISBN:978-1-4673-1836-5, pp: 1-5.

Strunz, K., E. Abbasi and D.N. Huu, 2014. DC microgrid for wind and solar power integration. IEEE. J. Emerging Sel. Topics Power Electron., 2: 115-126.

Tang, C.Y., Y. Guo and J.N. Jiang, 2011. Nonlinear dual-mode control of variable-speed wind turbines with doubly fed induction generators. IEEE. Trans. Control Syst. Technol., 19: 744-756.Uchida, K., T. Senjyu, N. Urasaki and A. Yona, 2009. Installation effect by solar heater system using solar radiation forecasting. Proceedings o f the 2009 Conference on Transmission and Distribution Exposition: Asia and Pacific, October 26-30, 2009, IEEE, Seoul, South Korea, ISBN:978-1-4244-5230-9, pp: 1-4.

Weimer, M.A., T.S. Paing and R.A. Zane, 2006. Remote area wind energy harvesting for low-power autonomous sensors. Proceedings of the 37th IEEE Conference on Power Electronics Specialists, June 18-22, 2006, Jeju, South Korea, ISBN:0-7803-9716-9, pp: 1-5.

Zhou, L. and D. Qu, 2006. Study of generalized predictive control scheme and algorithm based on artificial neural network. Proceedings of the 2006 IEEE International Conference on Information Acquisition, August 20-23, 2006, IEEE, Weihai, China, ISBN:1-4244-0528-9, pp: 1208-1212.